CHAPTER 3

STALL SPEED DETERMINATION

CHAPTER 3

STALL SPEED DETERMINATION

CHAPTER 3

FIGURES

CHAPTER 3

EQUATIONS

$$C_L = C_{L_{aero}} + \frac{T_G \sin \alpha_j}{q S} \quad \text{(Eq 3.12)} \quad 3.17$$

$$C_L = C_{L_{aero}} + \frac{T_G \sin \alpha_j}{\frac{n_z W}{C_L}} \quad \text{(Eq 3.13)} \quad 3.18$$

$$C_L = C_{L_{aero}} + C_L \left(\frac{T_G}{W} \frac{\sin \alpha_j}{n_z} \right) \quad \text{(Eq 3.14)} \quad 3.18$$

$$C_L \left(1 - \frac{T_G}{W} \frac{\sin \alpha_j}{n_z} \right) = C_{L_{aero}} \quad \text{(Eq 3.15)} \quad 3.18$$

$$C_L = \frac{C_{L_{aero}}}{\left(1 - \frac{T_G}{W} \frac{\sin \alpha_j}{n_z} \right)} \quad \text{(Eq 3.16)} \quad 3.18$$

$$C_L = f \left(C_{L_{aero}}, \frac{T_G}{W}, \sin \alpha_j, n_z \right) \quad \text{(Eq 3.17)} \quad 3.18$$

$$C_{L_{aero}} = f \left(\alpha, M, R_e \right) \quad \text{(Eq 3.18)} \quad 3.19$$

$$C_{L_{aero}} = \frac{n_z W}{q S} = \frac{n_z W}{\frac{\gamma}{2} P_{ssl} S \delta M^2} \quad \text{(Eq 3.19)} \quad 3.19$$

$$C_{L_{aero}} = \frac{n_z \left(\frac{W}{\delta} \right)}{\left(\frac{\gamma}{2} P_{ssl} S \right) M^2} \quad \text{(Eq 3.20)} \quad 3.19$$

$$V_s = V_{s_{Test}} \sqrt{\frac{R + 2}{R + 1}} \text{ (For decelerations)} \quad \text{(Eq 3.21)} \quad 3.21$$

$$C_{L_s} = C_{L_{Test}} \left(\frac{R + 1}{R + 2} \right) \text{ (For decelerations)} \quad \text{(Eq 3.22)} \quad 3.21$$

$$V_s = V_{s_{Test}} \sqrt{\frac{R + 1}{R + 2}} \text{ (For accelerations)} \qquad \text{(Eq 3.23)} \qquad 3.21$$

$$R = \frac{V_{s_{Test}}}{\frac{c}{2}\dot{V}} \qquad \text{(Eq 3.24)} \qquad 3.21$$

$$C_{L_{max}}{}_{Std\ \dot{V}} = C_{L_{max}} + K_d \left(\dot{V}_{Std} - \dot{V}_{Test} \right) \qquad \text{(Eq 3.25)} \qquad 3.22$$

$$C_{L_{max}}{}_{Std\ \dot{V},\ CG} = C_{L_{max}}{}_{Std\ \dot{V}} + K_c \left(CG_{Std} - CG_{Test} \right) \qquad \text{(Eq 3.26)} \qquad 3.25$$

$$\Delta L_t \left(l_t \right) = T_G (Z) - D_R (Y) \qquad \text{(Eq 3.27)} \qquad 3.26$$

$$\Delta C_{L_t} = \frac{T_G}{q S} \left(\frac{Z}{l_t} \right) - \frac{D_R}{q S} \left(\frac{Y}{l_t} \right) \qquad \text{(Eq 3.28)} \qquad 3.26$$

$$R_e = \frac{\rho V c}{\mu} = V_e \sqrt{\rho} \left(\frac{\sqrt{\rho_{ssl}}\ c}{\mu} \right) \qquad \text{(Eq 3.29)} \qquad 3.27$$

$$C_{T_G} = \frac{T_G \sin \alpha_j}{q S} \qquad \text{(Eq 3.30)} \qquad 3.29$$

$$C_{L_{max}}{}_{Std\ \dot{V},\ CG,\ W} = C_{L_{max}}{}_{Std\ \dot{V},\ CG} + K_W \left(W_{Std} - W_{Test} \right) \qquad \text{(Eq 3.31)} \qquad 3.31$$

$$V_i = V_o + \Delta V_{ic} \qquad \text{(Eq 3.32)} \qquad 3.36$$

$$V_c = V_i + \Delta V_{pos} \qquad \text{(Eq 3.33)} \qquad 3.36$$

$$H_{P_i} = H_{P_o} + \Delta H_{P_{ic}} \qquad \text{(Eq 3.34)} \qquad 3.36$$

$$H_{P_c} = H_{P_i} + \Delta H_{pos} \qquad \text{(Eq 3.35)} \qquad 3.36$$

$$n_{z_i} = n_{z_o} + \Delta n_{z_{ic}} \qquad \text{(Eq 3.36)} \qquad 3.36$$

$$n_z = n_{z_i} + \Delta n_{z_{tare}} \qquad \text{(Eq 3.37)} \qquad 3.36$$

$$C_{L_{max_{Test}}} = \frac{n_z \, W_{Test}}{0.7 \, P_{ssl} \, \delta_{Test} \, M^2 \, S} \qquad \text{(Eq 3.38)} \qquad 3.37$$

$$R = \frac{V_c}{\frac{c}{2}\dot{V}_{Test}} \qquad \text{(Eq 3.39)} \qquad 3.37$$

$$C_{L_{max_{Std\,\dot{V}}}} = C_{L_{max_{Test}}} \left(\frac{R + 1}{R + 2} \right) \qquad \text{(Eq 3.40)} \qquad 3.37$$

$$\left(C_{L_{aero_{Std\,\dot{V},\,CG,\,W}}} \right)_{Pwr\,ON} = \left(C_{L_{max_{Std\,\dot{V},\,CG,\,W}}} \right)_{Pwr\,ON} - C_{T_G} \qquad \text{(Eq 3.41)} \qquad 3.42$$

$$\left(C_{L_{aero_{Std\,\dot{V},\,CG,\,W}}} \right)_{Pwr\,OFF} = \left(C_{L_{aero_{Std\,\dot{V},\,CG,\,W}}} \right)_{Pwr\,ON} - \Delta C_{L_t} - \Delta C_{L_E} \qquad \text{(Eq 3.42)} \qquad 3.42$$

$$V_{e_s} = \sqrt{\frac{841.5 \, n_z \, W}{C_{L_{max}} \, S}} \qquad \text{(Eq 3.43)} \qquad 3.44$$

CHAPTER 3

STALL SPEED DETERMINATION

3.1 INTRODUCTION

This chapter deals with determining the stall airspeed of an airplane with emphasis on the takeoff and landing configurations. The stall is defined and factors which affect the stall speed are identified. Techniques to measure the stall airspeed are presented and data corrections for the test results are explained.

3.2 PURPOSE OF TEST

The purpose of this test is to determine the stall airspeed of the airplane in the takeoff and landing configuration, with the following objectives:

1. Determine the 1 g stall speed for an airplane at altitude and at sea level.
2. Apply corrections to obtain the stall speed for standard conditions to check compliance with performance guarantees.
3. Define mission suitability issues.

3.3 THEORY

The stall speed investigation documents the low speed boundary of the steady flight envelope of an airplane. In the classic stall, the angle of attack (α) is increased until the airflow over the wing surface can no longer remain attached and separates. The resulting abrupt loss of lift causes a loss of altitude and, in extreme cases, a loss of control. The operational requirement for low takeoff and landing airspeeds places these speeds very near the stall speed. Since the stall speed represents an important envelope limitation, it is a critical design goal and performance guarantee for aircraft procurement and certification trials. Verifying the guaranteed stall speed is a high priority early in the initial testing phases of an airplane. The significance of this measurement justifies the attention paid to the factors which affect the stall speed.

3.3.1 LOW SPEED LIMITING FACTORS

While defining the boundaries of the performance envelope, it is not uncommon to face degraded flying qualities near the limits. The reduced dynamic pressure near the stall airspeed produces a degradation in the effectiveness of the flight controls in addition to a lift reduction. Maintaining lift at these low speeds requires high α, which results in high drag and, frequently, handling difficulties. At some point in the deceleration, a minimum steady speed is reached which is ultimately defined by one of the following limiting factors:

1. Loss of lift. The separated flow is unable to produce sufficient lift.
2. Drag. Large increases in induced drag may cause high sink rates, compromising flight path control.
3. Uncommanded aircraft motions. These undesirable motions can range from a slight pitch over to a severe nose slice and departure.
4. Undesirable flying qualities. These characteristics include intolerable buffet level, shaking of the controls, wing rock, aileron reversal, and degraded stability.
5. Control effectiveness. Full nose up pitch control limits may be reached before any of the above conditions occurs.

From a test pilot's perspective, the task is to investigate how much lift potential can be exploited for operational use, without compromising aircraft control in the process. The definition of stall speed comes from that investigation. The 1 g stall case is discussed in this chapter and the accelerated stall case is covered in Chapter 6.

3.3.1.1 MAXIMUM LIFT COEFFICIENT

The discussion of minimum speed includes the notion of maximum lift coefficient ($C_{L_{max}}$). To maintain lift in a controlled deceleration at 1 g, the lift coefficient (C_L) increases as the dynamic pressure decreases (as a function of velocity squared). This increase in lift coefficient is provided by the steadily increasing α during the deceleration. At some point in the deceleration the airflow over the wing separates, causing a reduction of lift. The lift coefficient is a maximum at this point, and the corresponding speed at these conditions represents the minimum flying speed.

A high maximum lift coefficient is necessary for a low minimum speed. Wings designed for high speed are not well suited for high lift coefficients. Therefore, $C_{L_{max}}$ is

typically enhanced for the takeoff and landing configurations by employing high lift devices, such as flaps, slats, or other forms of boundary layer control (BLC). The determination of stall airspeed for the takeoff or landing configuration invariably involves some of these high lift devices.

While the wing is normally a predominant factor in determining minimum speed capability, the maximum lift capability frequently depends upon thrust and center of gravity (CG) location. Thrust may make significant contributions to lift through both direct and indirect effects. The location of the CG affects pitch control effectiveness, pitch stability, and corresponding tail lift (positive or negative lift) required to balance pitching moments. These effects can be significant for airplanes with high thrust to weight ratios or close coupled control configurations (short moment arm for tail lift).

3.3.1.2 MINIMUM USEABLE SPEED

The speed corresponding to $C_{L_{max}}$ may not be a reasonable limit. Any of the other potential limitations from paragraph 3.3.1 may prescribe a minimum useable speed which is higher than the speed corresponding to $C_{L_{max}}$. The higher speed may be appropriate due to high sink rate, undesirable motions, flying qualities, or control effectiveness limits. Influence of the separated flow on the empennage may cause instabilities, loss of control, or intolerable buffeting. Any of these factors could present a practical minimum airspeed limit at a lift coefficient less than the $C_{L_{max}}$ potential of the airplane. In this case, the classic stall is not reached and a minimum useable speed is defined by another factor.

3.3.2 DEFINITION OF STALL SPEED

The definition of stall airspeed is linked to the practical concept of minimum useable airspeed. Useable means controllable in the context of a mission task. The stall speed might be defined by the aerodynamic stall, or it might be defined by a qualitative controllability threshold. The particular controllability issue may be defined precisely, as in an abrupt g-break, or loosely, as in a gradual increase in wing rock to an unacceptable level. Regardless of the particular controllability characteristic in question, the stall definition must be as precise as possible so the stall speed measurement is consistent and repeatable. Throughout the aerospace industry the definition of stall embraces the same concept of minimum useable speed. Two examples are presented below:

"The stalling speed, if obtainable, or the minimum steady speed, in knots (CAS), at which the airplane is controllable with.... (the words that follow describe the required configuration)."

- FAR Part 23.45

"The stall speed (equivalent airspeed) at 1 g normal to the flight path is the highest of the following:

1. The speed for steady straight flight at $C_{L_{max}}$ (the first local maximum of lift coefficient versus α which occurs as C_L is increased from zero).
2. The speed at which uncommanded pitching, rolling, or yawing occurs.
3. The speed at which intolerable buffet or structural vibration is encountered."

- MIL-STD-1797A

If a subjective interpretation is required for the stall definition, the potential exists for disagreement, particularly between the manufacturer and the procuring agency. In cases where the stall definition rests on a qualitative opinion, it is important to be as precise as possible for consistent test results. For example, if the dominant characteristic is a progressively increasing wing rock, the stall might be defined by a particular amplitude of oscillation for consistency (perhaps ± 10 deg bank). The stall may also be defined by a minimum permissible airspeed based upon an excessive sinking speed, or the inability to perform altitude corrections or execute a waveoff. If the stall is based on a criteria other than decreased lift, the minimum speed is usually specified as a specific α limit. This α limit, with approval by the procuring agency, is used as the stall speed definition for all specification requirements.

The important point is the definitions of controllable and useable are made by the user. The test pilot should be aware of the contractual significance of his interpretations in defining the stall, but must base his stall definition solely on mission suitability requirements.

3.3.3 AERODYNAMIC STALL

3.3.3.1 FLOW SEPARATION

In the classic stall, the lift coefficient increases steadily until airflow separation occurs, resulting in a loss of lift. The separation may occur at various locations on the wing

and propagate in different patterns to influence the stall characteristics. Good characteristics generally result when the separation begins on the trailing edge of the wing root and progresses gradually forward and outboard. Separation at the wing tips is undesirable due to the loss of lateral control effectiveness and the tendency for large bank angle deviations when one tip stalls before the other. Separation at the leading edge is invariably abrupt, precipitating a dangerous loss of lift with little or no warning. Some wing characteristics which cause these variations in stall behavior are wing section, aspect ratio, taper ratio, and wing sweep.

3.3.3.2 WING SECTION

The relevant wing section design characteristics are airfoil thickness, thickness distribution, camber, and leading edge radius. To produce high maximum lift coefficients while maintaining the desirable separation at the trailing edge, the wing section must be designed to keep the flow attached at high α. Separation characteristics of two classes of wing section are shown in figure 3.1.

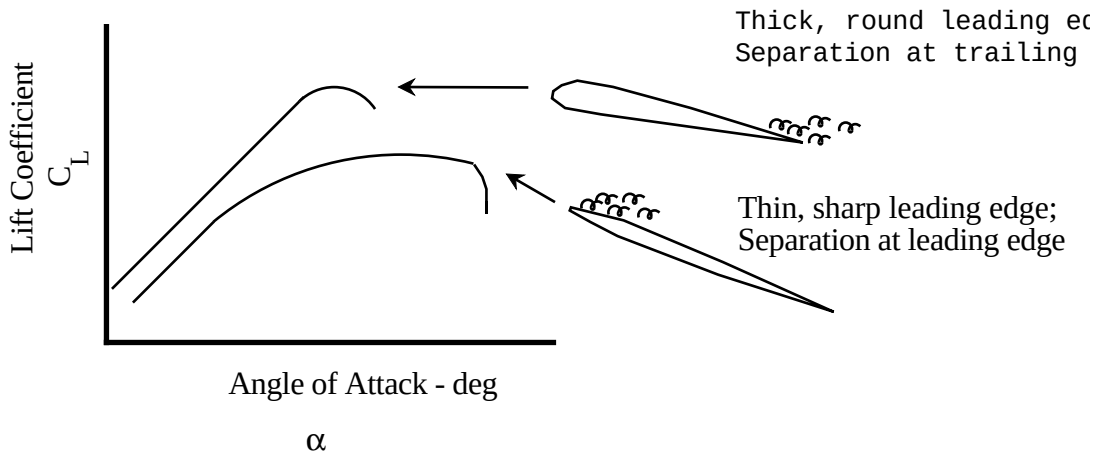

Figure 3.1
SAMPLE AIRFLOW SEPARATION CHARACTERISTICS

The classic airfoil shape features a relatively large leading edge radius and smoothly varying thickness along the chord line. This section is capable of producing large lift coefficients and promotes favorable airflow separation beginning at the trailing edge. The decrease in lift coefficient beyond $C_{L_{max}}$ is relatively gradual. Alternately, thin airfoils, particularly those with a small leading edge radius, typically have lower maximum lift

coefficients. Airflow separation is less predictable, often beginning at the wing leading edge. Lift coefficient can decrease abruptly near $C_{L_{max}}$, even for small increases in α, and may precipitate unusual attitudes if the flow separates unevenly from both wings. High drag approaching $C_{L_{max}}$ can result in insidious and potentially high sink rates.

3.3.3.2.1 ASPECT RATIO

Aspect ratio (AR) is defined as the wing span divided by the average chord, or alternately, the square of the wing span divided by the wing area. The effect of increasing aspect ratio is to increase $C_{L_{max}}$ and steepen the lift curve slope as shown in figure 3.2.

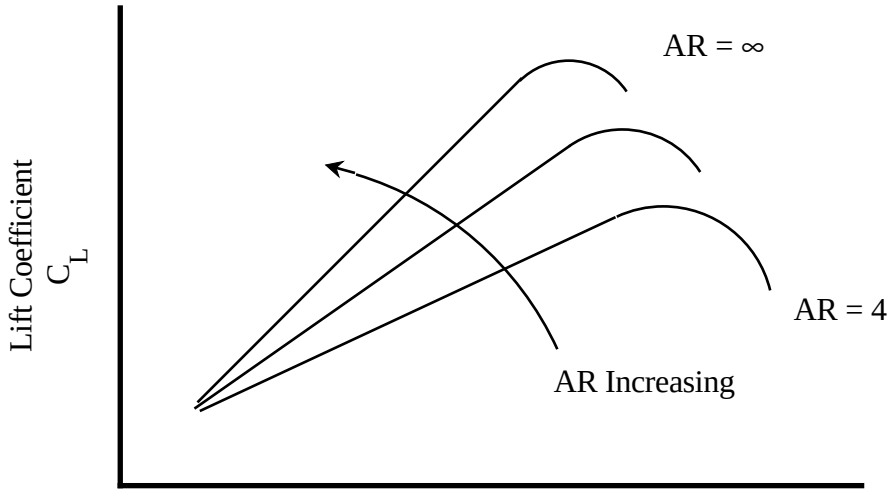

Figure 3.2
EFFECTS OF ASPECT RATIO

$C_{L_{max}}$ for a high aspect ratio wing occurs at a relatively low α, and corresponding low drag coefficient. Low aspect ratio wings, on the other hand, typically have shallow lift curve slopes and a relatively gradual variation of lift coefficient near $C_{L_{max}}$. The α for $C_{L_{max}}$ is higher, and the drag at these conditions is correspondingly higher.

3.3.3.2.2 TAPER RATIO

Taper ratio (λ) is the the chord length at the wing tip divided by the chord length at the wing root. For a rectangular wing ($\lambda = 1$), strong tip vortices reduce the lift loading at the tips. As the tip chord dimension is reduced, the tip loading increases, causing the adverse tendency for the wing tip to stall before the root. The tip stall typically causes a wing drop with little or no warning. The loss of lift is usually abrupt and controllability suffers with decreased aileron effectiveness.

3.3.3.2.3 WING SWEEP

The effect of increasing wing sweep angle (Λ) is to decrease the lift curve slope and $C_{L_{max}}$ as depicted in figure 3.3.

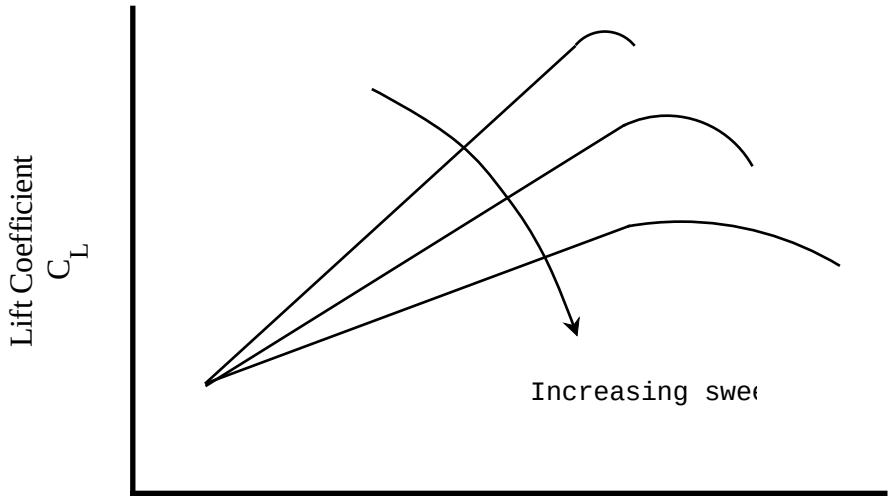

Figure 3.3
EFFECTS OF WING SWEEP

While the swept wing offers dramatic transonic drag reduction, the lift penalty at high α is substantial. As a wing is swept, $C_{L_{max}}$ decreases, according to the formula:

$$C_{L_{max\ (\Lambda)}} = C_{L_{max\ (\Lambda = 0)}} \cos(\Lambda) \qquad \text{(Eq 3.1)}$$

Where:

$C_{L_{max\ (\Lambda)}}$	Maximum lift coefficient at Λ wing sweep	
$C_{L_{max\ (\Lambda = 0)}}$	Maximum lift coefficient at $\Lambda = 0$	
Λ	Wing sweep angle	deg.

Wing sweep causes a spanwise flow and a tendency for the boundary layer to thicken, inducing a tip stall. Besides the lateral control problem caused by tip stall, the loss of lift at the wing tips causes the center of pressure to move forward, resulting in a tendency to pitch up at the stall. Delta wing configurations are particularly susceptible to this pitch up tendency. The tip stall is often prevented by blocking the spanwise flow, using stall fences (MiG-21) or induced vortices from a leading edge notch at mid-span (F-4). Forward sweep, as in the X-29, exhibits the characteristic spanwise flow, but the tendency in this case is for root stall, and a resulting pitch down tendency at the stall.

3.3.3.3 IMPROVING SEPARATION CHARACTERISTICS

The tip stall caused by adverse flow separation characteristics of wings with low AR, low λ, or high Λ is usually avoided in the design phase by inducing a root stall through geometric wing twist, varying the airfoil section along the span, or employing leading edge devices at the tips. If problems show up in the flight test phase, fixes are usually employed such as stall strips or some similar device to trip the boundary layer at the root as shown in figure 3.4.

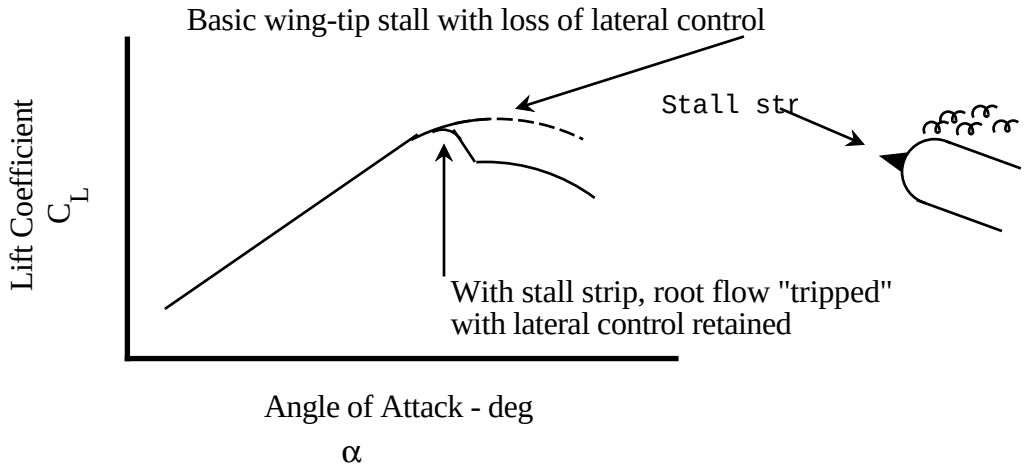

Figure 3.4
USE OF STALL STRIP AT WING ROOT

3.3.4 MAXIMUM LIFT

The previous section discussed factors which affect the shape of the lift curve at $C_{L_{max}}$ and the airflow separation characteristics at high α. These factors influence the airplane handling characteristics near $C_{L_{max}}$ and may prevent full use of the airplane's lift potential. Apart from handling qualities issues, low minimum speeds are achieved by designing for high maximum lift capability. The maximum lift characteristics of various airfoil sections are shown in figure 3.5.

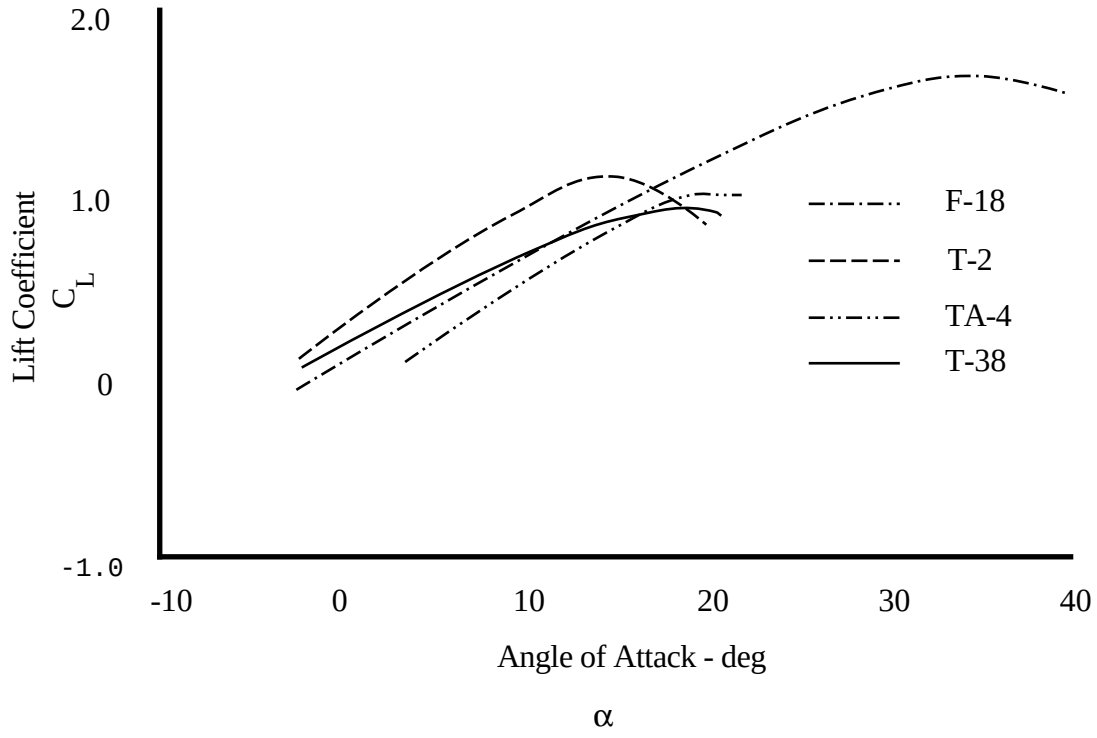

Figure 3.5
AIRFOIL SECTION LIFT CHARACTERISTICS

All of the airfoil sections displayed have roughly the same lift curve slope for low α, about 0.1 per deg. The theoretical maximum value is 2π per radian, or 0.11 per deg. The airfoil sections differ, however, at high α. The maximum value of lift coefficient and α where the maximum is reached determine the suitability of the airfoil for takeoff and landing tasks.

The desired low takeoff and landing speeds require high lift coefficients. The following expression illustrates the relationship between airspeed and lift coefficient:

$$V_{e_s} = \sqrt{\frac{n_z W}{C_{L_s} q S}} \qquad \text{(Eq 3.2)}$$

The potential benefit in stall speed reduction through increased lift coefficient can be seen in the following expression:

$$\frac{V_{e_{s_1}}}{V_{e_{s_2}}} = \sqrt{\frac{C_{L_{s_2}}}{C_{L_{s_1}}}} \qquad \text{(Eq 3.3)}$$

Large changes in lift coefficient are required in order to change equivalent airspeed (V_e) appreciably. Notice for a nominal 20% decrease in stall speed, over 50% increase in lift coefficient is required:

$$\text{If} \quad \frac{V_{e_{s_1}}}{V_{e_{s_2}}} = 0.8\,, \quad \text{then} \quad \frac{C_{L_{s_2}}}{C_{L_{s_1}}} = 0.64 \qquad \text{(Eq 3.4)}$$

And,

$$\frac{C_{L_{s_1}}}{C_{L_{s_2}}} = 1.56 \qquad \text{(Eq 3.5)}$$

Where:

C_{L_s}	Stall lift coefficient	
n_z	Normal acceleration	g
q	Dynamic pressure	psf
S	Wing area	ft^2
V_{e_s}	Stall equivalent airspeed	ft/s
W	Weight	lb.

Large lift coefficient increases are required to make effective decreases in stall speed. Since the wing design characteristics for high speed tasks are not compatible with those for high lift coefficient, the airplane designer must use high lift devices.

3.3.5 HIGH LIFT DEVICES

3.3.5.1 GENERATING EXTRA LIFT

Wing lift can be increased by using these techniques:

1. Increasing the wing area.
2. Increasing the wing camber.
3. Delaying the flow separation.

Various combinations of these techniques are employed to produce the high lift coefficients required for takeoff and landing tasks. Typical lift augmentation designs employ leading and trailing edge flaps and a variety of BLC schemes including slots, slats, suction and blowing, and the use of vortices. The relative benefit of each particular technique depends upon the lift characteristics of the wing on which it's used. For example, a trailing edge flap on a propeller airplane with a straight wing might increase $C_{L_{max}}$ three times as much as the same flap on a jet with a swept wing.

3.3.5.2 TRAILING EDGE FLAPS

Trailing edge flaps are employed to change the effective wing camber. They normally affect the aft 15% to 20% of the chord. The most common types of trailing edge flaps are shown in figure 3.6.

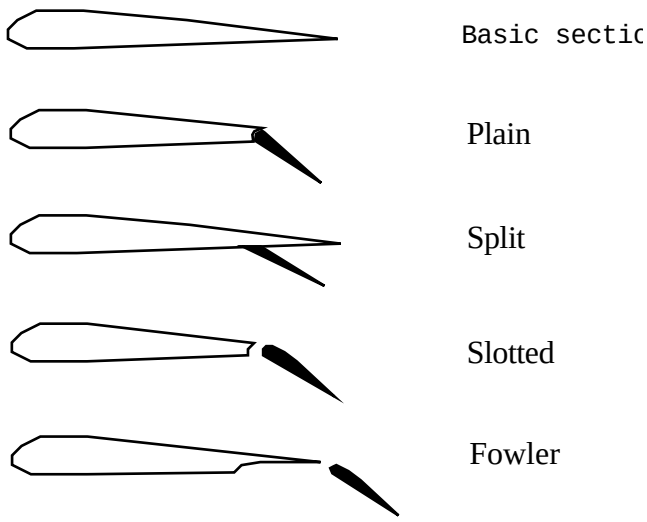

Figure 3.6
COMMON TRAILING EDGE FLAPS

The wing-flap combination behaves like a different wing, with characteristics dependent upon the design of the flap system. The plain flap is simply a hinged aft portion of the cross section of the wing, as used in the T-38. The split flap is a flat plate deflected from the lower surface of the wing, as in the TA-4. Slotted flaps direct high energy air over the upper flap surfaces to delay separation, as in the F-18 and U-21. Fowler flaps are slotted flaps which translate aft as they deflect to increase both the area of the wing and the camber, as in the T-2 and P-3. The relative effectiveness of the various types of trailing edge flaps is shown in figure 3.7.

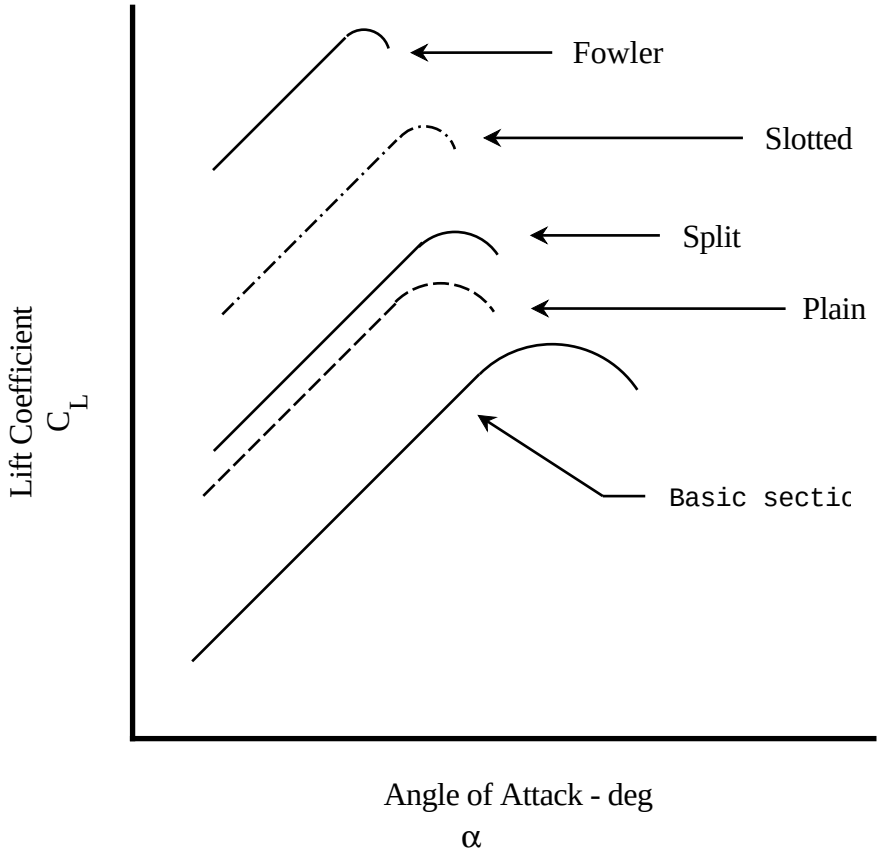

Figure 3.7
LIFT CHARACTERISTICS OF TRAILING EDGE FLAPS

All types provide a significant increase in $C_{L_{max}}$, without altering the lift curve slope. An added benefit is the reduction in the α for $C_{L_{max}}$, which helps the field of view over the nose at high lift conditions and reduces the potential for geometric limitations due to excessive α during takeoff and landing.

3.3.5.3 BOUNDARY LAYER CONTROL

Lift enhancement can be achieved by delaying the airflow separation over the wing surface. The boundary layer can be manipulated by airfoils or other surfaces installed along the wing leading edge. In addition, suction or blowing techniques can be employed at various locations on the wing to control or energize the boundary layer. Vortices are also employed to energize the boundary layer and delay airflow separation until a higher α. Different types of BLC are discussed in the following sections.

3.3.5.3.1 LEADING EDGE DEVICES

Leading edge devices are designed primarily to delay the flow separation until a higher α is reached. Some common leading edge devices are shown in figure 3.8.

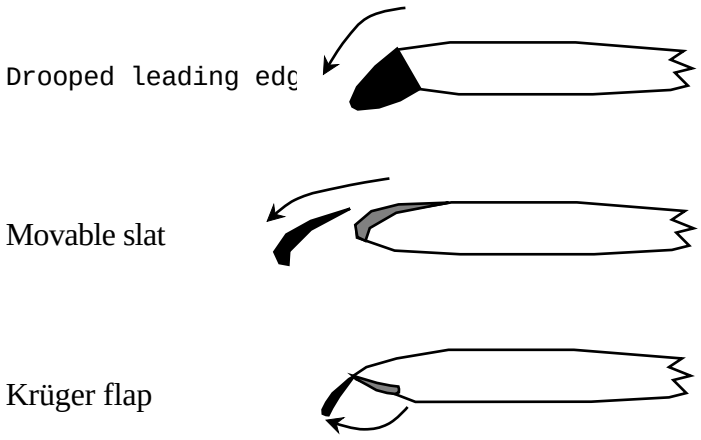

Figure 3.8
SAMPLE LEADING EDGE DEVICES

The lift provided from the leading edge surface is negligible; however, by helping the flow stay attached to the wing, flight at higher α is possible. An increase in $C_{L_{max}}$ is realized, corresponding to the lift resulting from the additional α available as shown in figure 3.9.

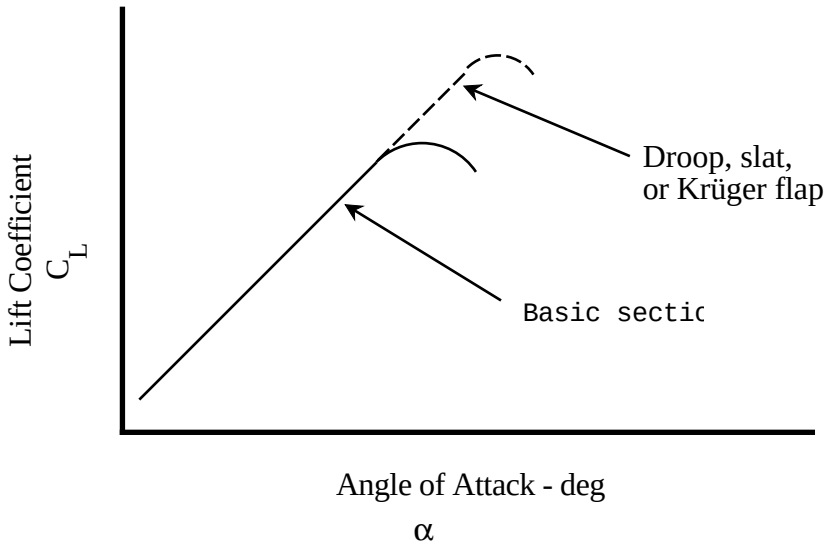

Figure 3.9
LEADING EDGE DEVICE EFFECTS

Since the α for $C_{L_{max}}$ may be excessively high, leading edge devices and slots are invariably used in conjunction with trailing edge flaps (except in delta wings) in order to reduce the α to values acceptable for takeoff and landing tasks.

3.3.5.3.2 BLOWING AND SUCTION

BLC can also involve various blowing or suction techniques. The concept is to prevent the stagnation of the boundary layer by either sucking it from the upper surface or energizing it, usually with engine bleed air. If BLC is employed on the leading edge, the effect is similar to a leading edge device. The energized flow keeps the boundary layer attached, allowing flight at higher α. If the high energy air is directed over the main part of the wing or a trailing edge flap (a blown wing or flap), the effect is similar to adding a trailing edge device. In either application if engine bleed air is used, the increase in lift is proportional to thrust.

3.3.5.3.3 VORTEX LIFT

Vortices can be used to keep the flow attached at extremely high α. Strakes in the F-16 and leading edge extensions in the F-18 are used to generate powerful vortices at high α. These vortices maintain high energy flow over the wing and make dramatic lift

improvements. Canard surfaces can be used to produce powerful vortices for lift as well as pitching moments for control, as in the Gripen, Rafale, European fighter aircraft, and X-31 designs.

3.3.6 FACTORS AFFECTING $C_{L_{MAX}}$

3.3.6.1 LIFT FORCES

To specify the airplane's maximum lift coefficient, it is necessary to examine the forces which contribute to lift. Consider the airplane in a glide as depicted in figure 3.10.

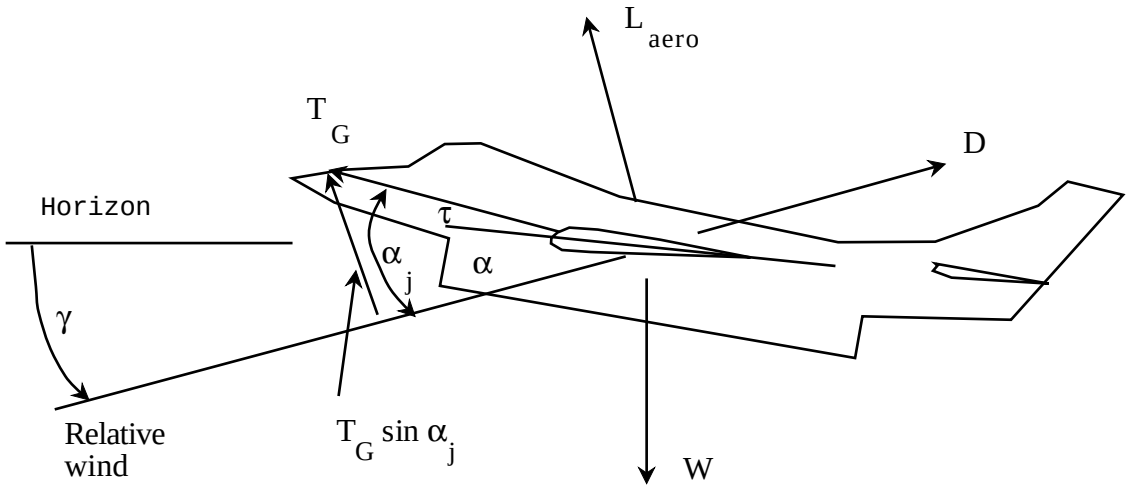

Figure 3.10
AIRPLANE IN STEADY GLIDE

Where:

α	Angle of attack	deg
α_j	Thrust angle	deg
D	Drag	lb
γ	Flight path angle	deg
L_{aero}	Aerodynamic lift	lb
τ	Inclination of the thrust axis with respect to the chord line	deg
T_G	Gross thrust	lb
W	Weight	lb.

Notice α_j can be expressed as:

$$\alpha_j = \alpha + \tau \qquad \text{(Eq 3.6)}$$

The total lift of the airplane is composed of aerodynamic lift (L_{aero}) and thrust lift (L_{Thrust}):

$$L = L_{aero} + L_{Thrust} \qquad \text{(Eq 3.7)}$$

Substituting the following expressions:

$$L = n_z W \qquad \text{(Eq 3.8)}$$

$$L_{Thrust} = T_G \sin \alpha_j \qquad \text{(Eq 3.9)}$$

The total lift is written:

$$L = n_z W = L_{aero} + T_G \sin \alpha_j \qquad \text{(Eq 3.10)}$$

Dividing by the product of dynamic pressure and wing area, qS, we get the expression for lift coefficient:

$$C_L = \frac{L}{q S} = \frac{n_z W}{q S} = \frac{L_{aero}}{q S} + \frac{T_G \sin \alpha_j}{q S} \qquad \text{(Eq 3.11)}$$

Or:

$$C_L = C_{L_{aero}} + \frac{T_G \sin \alpha_j}{q S} \qquad \text{(Eq 3.12)}$$

Substituting the following into Eq 3.12:

$$q S = \frac{n_z W}{C_L}$$

Results in:

$$C_L = C_{L_{aero}} + \frac{T_G \sin \alpha_j}{\frac{n_z W}{C_L}} \qquad \text{(Eq 3.13)}$$

Rearranging:

$$C_L = C_{L_{aero}} + C_L \left(\frac{T_G}{W} \frac{\sin \alpha_j}{n_z} \right) \qquad \text{(Eq 3.14)}$$

$$C_L \left(1 - \frac{T_G}{W} \frac{\sin \alpha_j}{n_z} \right) = C_{L_{aero}} \qquad \text{(Eq 3.15)}$$

Finally:

$$C_L = \frac{C_{L_{aero}}}{\left(1 - \frac{T_G}{W} \frac{\sin \alpha_j}{n_z} \right)} \qquad \text{(Eq 3.16)}$$

Eq 3.16 can be expressed functionally:

$$C_L = f \left(C_{L_{aero}}, \frac{T_G}{W}, \sin \alpha_j, n_z \right) \qquad \text{(Eq 3.17)}$$

Where:

α	Angle of attack	deg
α_j	Thrust angle	deg
C_L	Lift coefficient	
$C_{L_{aero}}$	Aerodynamic lift coefficient	
L	Lift	lb
L_{aero}	Aerodynamic lift	lb
L_{Thrust}	Thrust lift	lb
n_z	Normal acceleration	g
q	Dynamic pressure	psf

S	Wing area	ft^2
T_G	Gross thrust	lb
τ	Inclination of the thrust axis with respect to the chord line	deg
W	Weight	lb.

C_L changes in any of the above factors affect the total lift coefficient and must be accounted for in the determination of stall speed. The effects of each of these factors are developed in the following sections.

3.3.6.2 AERODYNAMIC LIFT COEFFICIENT

3.3.6.2.1 BASIC FACTORS

The aerodynamic lift coefficient is affected by many factors. From dimensional analysis we get the result:

$$C_{L_{aero}} = f\left(\alpha, M, R_e\right) \qquad \text{(Eq 3.18)}$$

As long as the thrust contributions are negligible and the airplane is in steady flight, the lift coefficient is specified by α, Mach, and R_e. The expression for $C_{L_{aero}}$ is:

$$C_{L_{aero}} = \frac{n_z W}{q S} = \frac{n_z W}{\frac{\gamma}{2} P_{ssl} S \delta M^2} \qquad \text{(Eq 3.19)}$$

Rearranging:

$$C_{L_{aero}} = \frac{n_z\left(\frac{W}{\delta}\right)}{\left(\frac{\gamma}{2} P_{ssl} S\right) M^2} \qquad \text{(Eq 3.20)}$$

Where:

α	Angle of attack	deg
$C_{L_{aero}}$	Aerodynamic lift coefficient	
δ	Pressure ratio	

γ	Ratio of specific heats	
M	Mach number	
n_z	Normal acceleration	g
$n_z \frac{W}{\delta}$	Referred normal acceleration	g-lb
P_{ssl}	Standard sea level pressure	2116.217 psf
q	Dynamic pressure	psf
R_e	Reynold's number	
S	Wing area	ft^2
W	Weight	lb.

Eq 3.20 shows $C_{L_{aero}}$ is a function of just $n_z \frac{W}{\delta}$ and Mach, if thrust and R_e effects are neglected. For power-off or partial power stalls at 10,000 ft and below, these assumptions are reasonable and there is good correlation when plotting $n_z \frac{W}{\delta}$ versus Mach.

However, significant contributions can come from deceleration rate, CG position, and indirect power effects, to alter the apparent value of $C_{L_{aero}}$. These effects, plus the influence of R_e, are discussed in the following sections.

3.3.6.2.2 DECELERATION RATE

Deceleration rate has a pronounced affect on lift coefficient. Changes to the flow pattern within 25 chord lengths of an airfoil have been shown to produce significant non-steady flow effects. The lift producing flow around the airfoil (vorticity) does not change instantaneously. During rapid decelerations the wing continues to produce lift for some finite time after the airspeed has decreased below the steady state stall speed. The measured stall speed for these conditions is lower than the steady state stall speed. For this reason, a deceleration rate not to exceed 1/2 kn/s normally is specified when determining steady state stall speed for performance guarantees.

To correct the test data for deceleration rate, an expression is used which relates the observed stall speed, the actual steady state stall speed, and R, a parameter which represents the number of chord lengths ahead of the wing the airflow change is affecting. The equation comes from reference 7, and pertains to the deceleration case alone:

$$V_s = V_{s_{Test}} \sqrt{\frac{R+2}{R+1}} \text{ (For decelerations)} \qquad \text{(Eq 3.21)}$$

If the deceleration rate is low, it takes a long time to make a velocity change, during which time the wing travels many semi-chord lengths. R is a large number, and V_s and $V_{s_{Test}}$ are nearly equal. High deceleration rates make R a small number, so V_s could be significantly larger then the test value. In terms of C_L, the deceleration correction is:

$$C_{L_s} = C_{L_{Test}} \left(\frac{R+1}{R+2} \right) \text{ (For decelerations)} \qquad \text{(Eq 3.22)}$$

A similar analysis holds for errors due to accelerations, except the measured stall speeds are higher than steady state values. This case is applicable to the takeoff phase, and especially for catapult launches. The expression for accelerations is similar to Eq 3.22:

$$V_s = V_{s_{Test}} \sqrt{\frac{R+1}{R+2}} \text{ (For accelerations)} \qquad \text{(Eq 3.23)}$$

The R parameter came from wind tunnel tests, and is hard to relate to flight tests. However, experimental results lend credibility to the following empirical expression for R from reference 7:

$$R = \frac{V_{s_{Test}}}{\frac{c}{2}\dot{V}} \qquad \text{(Eq 3.24)}$$

Where:

$\frac{c}{2}$	Semi-chord length	ft
C_{L_s}	Stall lift coefficient	
$C_{L_{Test}}$	Test lift coefficient	
$\dot{V}$	Acceleration/deceleration rate	kn/s
R	Number of semi-chord lengths	
V_s	Stall speed	kn
$V_{s_{Test}}$	Test stall speed	kn.

An alternate approach to the deceleration correction involves plotting the test data for several values of deceleration rate. The steady state value, or the value at a specification deceleration rate, can be obtained by extrapolation or interpolation of the test results. Figure 3.11 illustrates the technique.

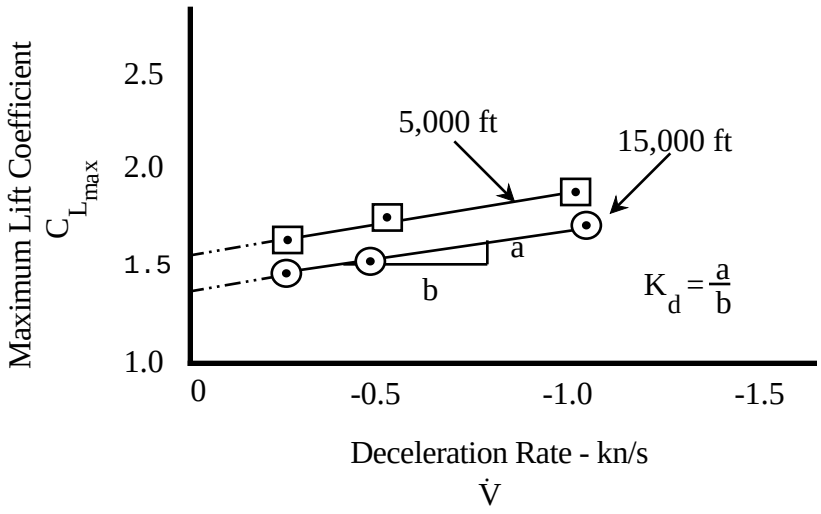

Figure 3.11
VARIATION OF $C_{L_{max}}$ WITH DECELERATION RATE

The data are faired to obtain the general correction represented by the slope of the line. Data can be corrected using the expression:

$$C_{L_{max}}{}_{Std\ \dot{V}} = C_{L_{max}} + K_d \left(\dot{V}_{Std} - \dot{V}_{Test} \right) \qquad \text{(Eq 3.25)}$$

Where:

$C_{L_{max}}$	Maximum lift coefficient	
$C_{L_{max}\ Std\ \dot{V}}$	Maximum lift coefficient at standard deceleration rate	
K_d	Slope of $C_{L_{max}}$ vs $\dot{V}$ (a negative number)	
$\dot{V}_{Std}$	Standard acceleration/deceleration rate	kn/s
$\dot{V}_{Test}$	Test acceleration/deceleration rate	kn/s.

If data using several deceleration rates are plotted, the corrections have a relatively high confidence level since no empirical expressions (as in the expression for R) are introduced.

3.3.6.2.3 CENTER OF GRAVITY EFFECTS

The CG affects the aerodynamic lift by altering the tail lift component. Consider the typical stable conditions where the CG is ahead of the aerodynamic center and the horizontal tail is producing a download. Moving the CG forward produces a nose down pitching moment, requiring more download to balance as shown in figure 3.12.

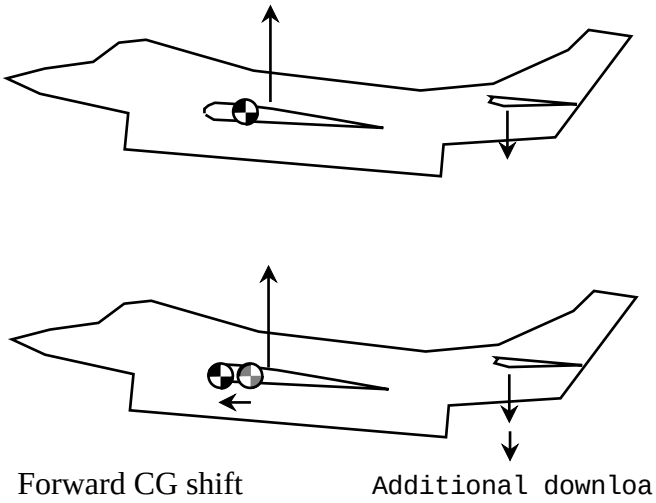

Figure 3.12
ADDITIONAL DOWNLOAD WITH FORWARD CG

The increased download to balance forward CG locations requires more nose up pitch control. In some cases, full aft stick (or yoke) is insufficient to reach the α for $C_{L_{max}}$, and a flight control deflection limit sets the minimum speed. Even if the tail is producing positive lift, as is the case with a negative static margin, the same effect prevails. In such cases, a forward CG shift would produce a decrease in the upload at the tail as shown in figure 3.13.

Thus, relatively aft CG locations have higher aerodynamic lift potential, resulting in lower airspeeds for any particular α. Forward CG locations have correspondingly higher speeds. The CG effect can be sizeable, particularly in designs with close-coupled, large horizontal control surfaces, like the Tornado or the F-14. For this reason, the stall speed requirement is frequently specified at the forward CG limit.

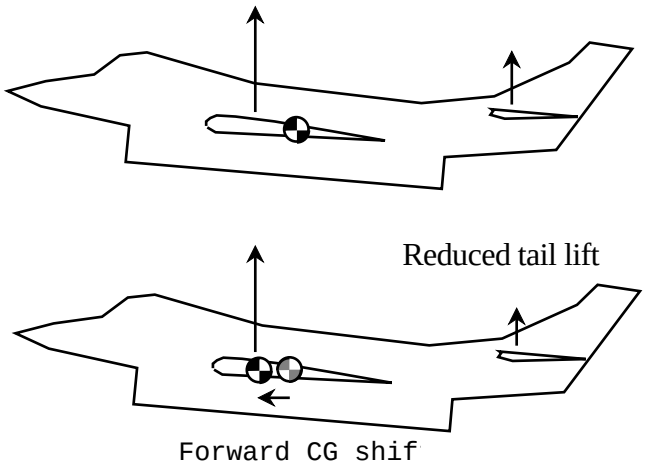

Figure 3.13
REDUCED LIFT WITH FORWARD CG SHIFT

To correct test data for the CG effects, plot $C_{L_{max\ Std\ \dot{V}}}$ versus CG_{Test} as in figure 3.14.

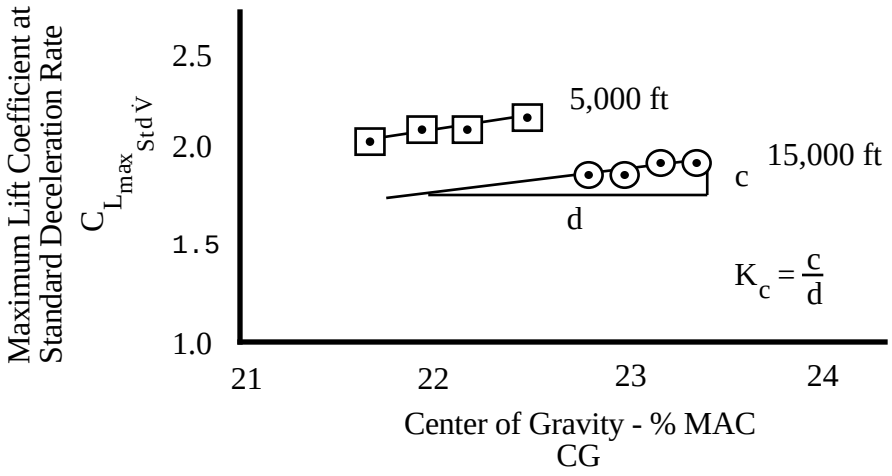

Figure 3.14
VARIATION OF $C_{L_{max}}$ WITH CG

$C_{L_{max}}$ increases as CG position increases in % MAC (CG moves aft). The correction is applied as follows:

$$C_{L_{max}}{}_{Std\,\dot{V},\,CG} = C_{L_{max}}{}_{Std\,\dot{V}} + K_c \left(CG_{Std} - CG_{Test} \right) \qquad \text{(Eq 3.26)}$$

Where:

CG_{Std}	Standard CG	% MAC
CG_{Test}	Test CG	% MAC
$C_{L_{max\ Std\,\dot{V}}}$	Maximum lift coefficient at standard deceleration rate	
$C_{L_{max\ Std\,\dot{V}\,,\,CG}}$	Maximum lift coefficient at standard deceleration rate and CG	
K_c	Slope of $C_{L_{max\ Std\,\dot{V}}}$ vs CG (positive number).	

3.3.6.2.4 INDIRECT POWER EFFECTS

There are two indirect power effects to consider: trim lift from thrust-induced pitching moments, and induced lift from flow entrainment. Both are straightforward to visualize, but difficult to measure. The calculations require data from the aircraft contractor.

Pitching Moment

Pitching moments are produced from ram drag (D_R) at the engine inlet and from gross thrust (T_G) where the thrust axis is inclined to the flight path as depicted in figure 3.15.

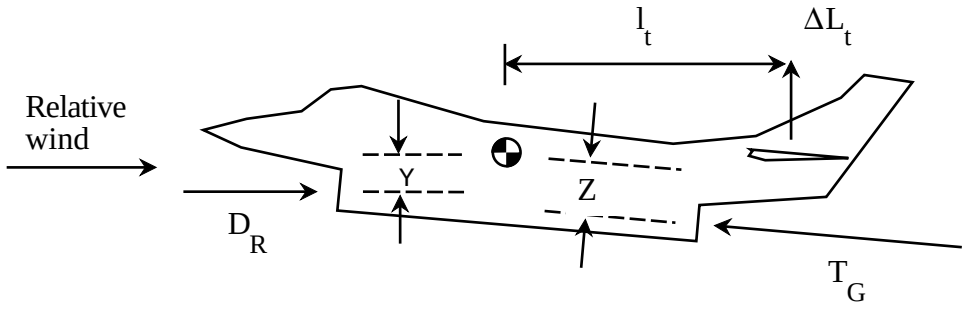

Figure 3.15
PITCHING MOMENTS FROM THRUST

Where:

ΔL_t	Tail lift increment	lb
D_R	Ram drag	lb
l_t	Moment arm for tail lift	ft
T_G	Gross thrust	lb
Y	Height of CG above ram drag	ft
Z	Height of CG above gross thrust	ft.

For this case, the moments from D_R and T_G require a balancing tail lift increment (ΔL_t), according to the expression:

$$\Delta L_t \left(l_t \right) = T_G \, (Z) - D_R \, (Y) \qquad \text{(Eq 3.27)}$$

The effect of ΔL_t on the aerodynamic lift coefficient is expressed as:

$$\Delta C_{L_t} = \frac{T_G}{q\,S}\left(\frac{Z}{l_t}\right) - \frac{D_R}{q\,S}\left(\frac{Y}{l_t}\right) \qquad \text{(Eq 3.28)}$$

Where:

ΔC_{L_t}	Incremental tail lift coefficient	
ΔL_t	Tail lift increment	lb
D_R	Ram drag	lb
l_t	Moment arm for tail lift	ft
q	Dynamic pressure	psf
S	Wing area	ft^2
T_G	Gross thrust	lb
Y	Height of CG above ram drag	ft
Z	Height of CG above gross thrust	ft.

This thrust effect is similar to the CG effect, except that the tail lift component is changed. The thrust axis component, T_G (Z), varies with thrust and CG location (especially vertical position), but is independent of α. The ram drag term, D_R (Y), varies with thrust, CG location, and α.

Thrust Induced Lift

If the nozzle is positioned so the exhaust induces additional airflow over a lifting surface, then an incremental lift is produced as a function of power setting. This effect is noticeable in designs where the nozzle is placed near the trailing edge of the wing, as in the A-6. At high thrust settings, and low airspeeds in particular, the jet exhaust causes increased flow over the wing, which raises the lift coefficient.

3.3.6.2.5 ALTITUDE

The effect of altitude on lift coefficient is due primarily to Reynold's number (R_e), which is defined below:

$$R_e = \frac{\rho V c}{\mu} = V_e \sqrt{\rho} \left(\frac{\sqrt{\rho_{ssl}}\ c}{\mu} \right) \qquad \text{(Eq 3.29)}$$

Where:

c	Chord length	ft
μ	Viscosity	lb-s/ft^2
ρ	Air density	slug/ft^3
R_e	Reynold's number	
ρ_{ssl}	Standard sea level air density	0.0023769 slug/ft^3
V	Velocity	kn
V_e	Equivalent airspeed	kn.

For the same V_e, R_e decreases with altitude. Results show as R_e decreases, the boundary layer has typically less energy and separates from the airfoil earlier than it would at lower altitude. Values of lift coefficient for α beyond this separation point are less than would be experienced at lower altitudes. R_e effects are depicted in figure 3.16.

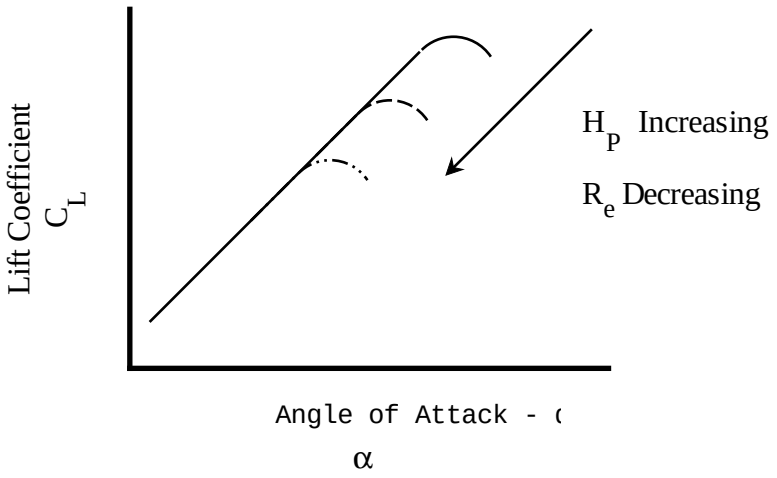

Figure 3.16
REYNOLD'S NUMBER EFFECT

The R_e effect of altitude on stall speed is on the order of 2 kn per 5,000 ft. To correct test data, or to refer test results to another altitude, the usual procedure is to plot $C_{L_{max}}$ versus H_{P_c}, using at least two different altitudes. Corrections to $C_{L_{max}}$ for standard deceleration rate, CG, and gross weight are made before plotting the variation with altitude. A typical plot is shown in figure 3.17.

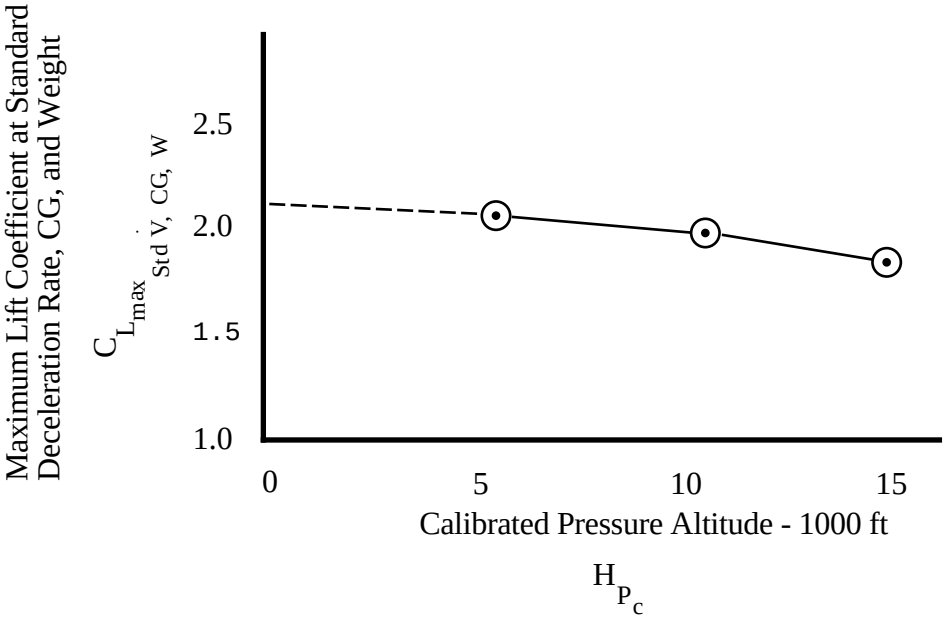

Figure 3.17
VARIATION OF $C_{L_{max}}$ WITH ALTITUDE

Figure 3.17 defines $C_{L_{max}}$ corrected to specific conditions of deceleration rate, CG, and weight for the standard altitude of interest. For extrapolations to sea level, data from three altitudes are recommended, since the variation is typically nonlinear.

3.3.6.3 THRUST AXIS INCIDENCE

The next factor to be developed in the lift equation is the component of thrust perpendicular to the flight path. Recall from Eq 3.7 direct thrust lift was accounted for in the development of the expression for total lift. Figure 3.18 highlights the thrust component of lift.

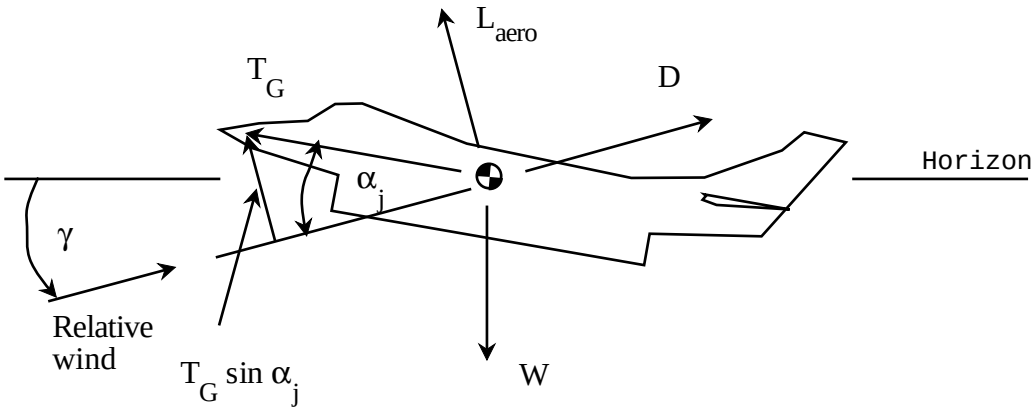

Figure 3.18
THRUST COMPONENT OF LIFT

The coefficient of thrust lift is denoted by the term C_{T_G} and is defined as:

$$C_{T_G} = \frac{T_G \sin \alpha_j}{q S} \qquad \text{(Eq 3.30)}$$

Where:

α_j	Thrust angle	deg
C_{T_G}	Coefficient of gross thrust lift	
q	Dynamic pressure	psf
S	Wing area	ft^2
T_G	Gross thrust	lb.

At high α and high thrust the thrust component of lift can be significant and must be accounted for in determining $C_{L_{max}}$ for minimum airspeed. The incidence of the nozzles may be fixed, as in conventional airplanes, or variable as in the Harrier or the YF-22. For aircraft designed to produce a large amount of thrust lift, the nozzle incidence angle is large, as is the thrust level. The thrust component is negligible, however, when the thrust is low or the incidence angle is small.

3.3.6.4 THRUST TO WEIGHT RATIO

The inclination of the thrust axis makes the actual thrust level significant in the measurement of airplane lift coefficient. Eq 3.16, repeated here for convenience, shows the thrust-to-weight term in the denominator, multiplied by the sine of the thrust axis inclination angle.

$$C_L = \frac{C_{L_{aero}}}{\left(1 - \frac{T_G}{W}\frac{\sin \alpha_j}{n_z}\right)} \qquad \text{(Eq 3.16)}$$

If the angle is large, then the test thrust-to-weight ratio can have a pronounced affect upon the results. This term is significant in power-on stalls for designs with high α capability, notably delta wing configurations where trailing edge flaps are not feasible. Corrections to test data for the effects of weight are significant only when the thrust-to-weight ratio at the test conditions is high, as in the takeoff or waveoff configurations. Plot $C_{L_{max}}$ versus gross weight to determine if a correction is necessary, as in figure 3.19.

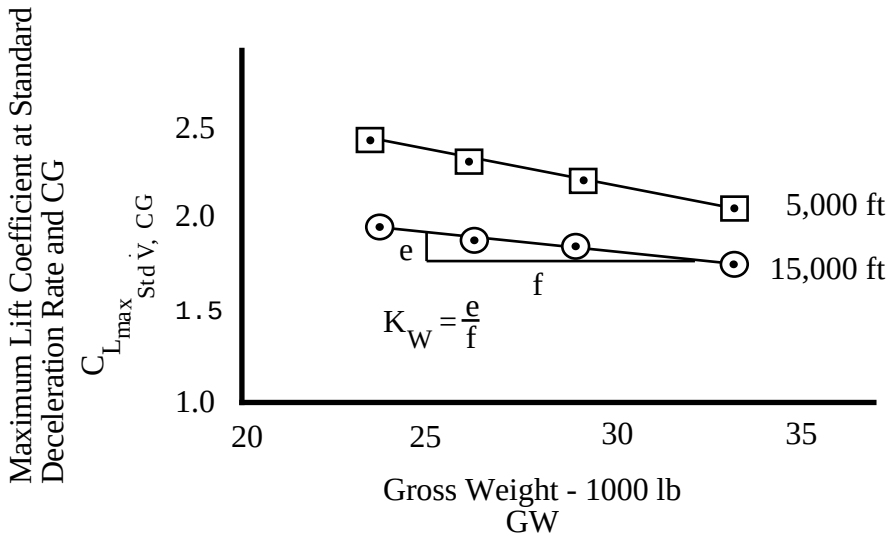

Figure 3.19
VARIATION OF $C_{L_{max}}$ WITH GROSS WEIGHT

If the graph has an appreciable slope, apply a gross weight correction as follows:

$$C_{L_{max}}{}_{Std\,\dot{V},\,CG,\,W} = C_{L_{max}}{}_{Std\,\dot{V},\,CG} + K_W \left(W_{Std} - W_{Test} \right) \qquad \text{(Eq 3.31)}$$

Where:

α_j	Thrust angle	deg
C_L	Lift coefficient	
$C_{L_{aero}}$	Aerodynamic lift coefficient	
$C_{L_{max\ Std\,\dot{V},\,CG}}$	Maximum lift coefficient at standard deceleration rate and CG	
$C_{L_{max\ Std\,\dot{V},\,CG,\,W}}$	Maximum lift coefficient at standard deceleration rate, CG, and weight	
K_W	Slope of $C_{L_{max\ Std\,\dot{V},\,CG}}$ vs GW (negative number)	lb^{-1}
n_z	Normal acceleration	g
T_G	Gross thrust	lb
W	Weight	lb
W_{Std}	Standard weight	lb
W_{Test}	Test weight	lb.

3.4 TEST METHODS AND TECHNIQUES

3.4.1 GRADUAL DECELERATION TECHNIQUE

For this technique a steady, gradual deceleration is maintained using the pitch control to modulate the deceleration rate until a stall occurs. Normally, the stall is indicated by a pitch down or a wing drop. A typical scope of test contains gradual decelerations for two CG locations using at least two test altitudes.

3.4.1.1 TEST PLANNING CONSIDERATIONS

While developing the test plan to determine the stall speed, consider the following issues:

1. Configuration. Define the precise configuration for the test, normally in accordance with a specification. Specify the following:

   a. Position of all high lift or drag devices.
   b. Trim setting.
   c. Thrust setting.
   d. Automatic flight control system (AFCS) status.

2. Weight and CG. Identify critical CG locations for the tests. Normally, the forward CG limit is critical if the stall is determined by $C_{L_{max}}$. Plan to get data at the specification gross weight, or use gross weight representative of mission conditions.

3. Loadings. Specify external stores loading. Stall speeds normally increase if external stores are loaded. Stores loading may have an adverse effect on stall and recovery characteristics.

4. Stall Characteristics. Consider the stall characteristics of the the test airplane. Plan build up tests if the stall characteristics are unknown or the pilot has no recent experience with stalls in the test airplane. Consider build up tests to determine the altitude required to recover from the stall. Employ appropriate safety measures to avoid inadvertent departures or post-stall gyrations. Specify recovery procedures for these cases.

5. Altitudes. Plan to get data at two or more test altitudes to allow for extrapolation of test results to sea level. Choose the lowest altitude based upon any adverse stall characteristics and predicted altitude lost during recoveries. Document the stall at an altitude approximately ten thousand feet above this minimum, and follow with tests at the lower altitude.

3.4.1.2 INSTRUMENTATION REQUIREMENTS

Precise accelerometers are necessary for accurate stall speed measurements. Twin-axis accelerometers for n_z and n_x are ideal, but it is impractical to align the accelerometers with the flight path at the stall. An n_x accelerometer could be used to measure deceleration rate accurately, except n_x is extremely sensitive to pitch attitude (θ) changes through the weight component, $W \sin\theta$. Record the n_z instrument error at 1 g for the test airplane to use in determining the tare correction. These tests are at essentially 1 g, but the changing θ and γ during the deceleration make the actual acceleration normal to the flight path difficult to determine. The precise n_z is determined by correcting the observed n_z using the alignment angle of the accelerometer with the fuselage reference line and the corrected α.

Angle of attack is normally obtained from a boom installation, to place the α vane in the free stream. Even with boom installations, however, corrections are required due to the upwash effect. These calibrations require comparisons of stabilized θ and flight path. Inertial navigation systems can be used for these measurements.

The measurement of airspeed is the biggest challenge. A calibrated trailing cone is a good source of airspeed data and can be used to calibrate the test airplane pitot static system. A pacer aircraft with a calibrated airspeed system is another option. The least accurate alternative is the pitot static system of the test airplane, since position error calibrations normally don't include the stall speed region.

If possible, obtain time histories of airspeed, n_z, θ, α, and pitch control position for analysis. Real time observations of flight parameters are not nearly as accurate. Buffet makes the gauges hard to read at a glance and it is difficult to time-correlate the critical readings to the actual stall event.

Reliable fuel weight at each test point is required. Normally, a precise fuel gauge calibration or fuel counter is used.

If power-on stalls are required and thrust effects are anticipated, maintenance personnel should trim the engine(s) prior to the tests.

Perform a weight and balance calibration for the test airplane after all test instrumentation is installed.

3.4.1.3 FLIGHT PROCEDURES

3.4.1.3.1 BUILD UP

Plan a build up sequence consisting of approaches to stall and recoveries using the standard recovery procedures. If telemetry is used or a pacer airplane is employed, an additional build up is recommended to practice the data retrieval procedures and identify any equipment, instrumentation, or coordination problems. Perform these build up procedures at a safe altitude prior to any performance tests.

3.4.1.3.2 DATA RUNS

Trim for approximately 1.2 times the predicted stall speed, which is typically very close to predicted optimum α for takeoffs and landings. Set the thrust appropriate for the configuration. Record the trim conditions, including trim settings. If applicable, position the pacer aircraft and have telemetry personnel ready.

From the trim speed, begin a steady 1/2 kn/s deceleration by increasing the pitch attitude. Control deceleration rate throughout the run by adjusting the pitch attitude. Attempt to fly a steady flight path, making all corrections smoothly to minimize n_z variations. When the stall is reached, record the data.

If telemetry is being used, make an appropriate “standby” call a few seconds before marking the stall. For tests involving a pacer airplane, the pacer stays with the test airplane throughout the deceleration. If the pacer tends to overrun the test airplane during the run, the pacer maintains fore-and-aft position by climbing slightly. The pacer stabilizes relative motion at the “standby” call. If there is any apparent relative motion when “mark” is called, the pacer notes it on the data card. The pacer keeps his eyes on the test airplane throughout

the stall and recovery to maintain a safe distance and to facilitate the join up following the test run.

Exercise care to recover from the stall in a timely manner, using the recommended recovery procedures. The perishable data are the airspeed and altitude at the stall. These numbers can be memorized and recorded after the recovery, together with the remaining less perishable entries.

3.4.1.4 DATA REQUIRED

Run number, Configuration, V_o, H_{P_o}, n_{z_o}, W, and α, Fuel used or fuel remaining. For power-on stalls, add N, OAT, and fuel flow.

3.4.1.5 TEST CRITERIA

1. Constant trim and thrust.
2. Coordinated, wings level flight.
3. Constant normal acceleration.
4. Less than 1 kn/s deceleration rate (1/2 kn/s is the normal target deceleration rate).

3.4.1.6 DATA REQUIREMENTS

1. If automatic data recording is available, record the 30 s prior to stall.
2. Steady deceleration rate for 10 s prior to stall.
3. $V_o \pm 1/2$ kn.
4. H_{P_o} as required for 2% accuracy for $\frac{W}{\delta}$.
5. $n_{z_o} \pm 0.05$ g, (nearest tenth).

3.4.1.7 SAFETY CONSIDERATIONS

Exercise due care and vigilance since all stall tests are potentially dangerous. Carefully consider crew coordination while planning recoveries and procedures for all contingencies, including:

1. Inadvertent departure.
2. Unintentional spin.
3. Engine flameout and air start.
4. Asymmetric power at high α.

Make appropriate weather limitations for the tests. List all necessary equipment for the tests and set go/no-go criteria. Identify critical airplane systems and make data card entries to prompt the aircrew to monitor these systems during the tests. Assign data taking and recording responsibilities for the flight. Stress lookout doctrine and consider using reserved airspace for high workload tests. Plan to initiate recovery at the stall, and record hand-held data after the recovery is complete.

3.5 DATA REDUCTION

3.5.1 POWER-OFF STALLS

Test results are normally presented as the variation of stall speed with gross weight. Another useful presentation is the variation of referred normal acceleration $\left(n_z \frac{W}{\delta}\right)$ with Mach. The following equations are used for power-off stall data reduction:

$$V_i = V_o + \Delta V_{ic} \qquad \text{(Eq 3.32)}$$

$$V_c = V_i + \Delta V_{pos} \qquad \text{(Eq 3.33)}$$

$$H_{P_i} = H_{P_o} + \Delta H_{P_{ic}} \qquad \text{(Eq 3.34)}$$

$$H_{P_c} = H_{P_i} + \Delta H_{pos} \qquad \text{(Eq 3.35)}$$

$$n_{z_i} = n_{z_o} + \Delta n_{z_{ic}} \qquad \text{(Eq 3.36)}$$

$$n_z = n_{z_i} + \Delta n_{z_{tare}} \qquad \text{(Eq 3.37)}$$

$$C_{L_{max_{Test}}} = \frac{n_z \, W_{Test}}{0.7 \, P_{ssl} \, \delta_{Test} \, M^2 \, S} \qquad \text{(Eq 3.38)}$$

$$R = \frac{V_c}{\frac{c}{2}\dot{V}_{Test}} \qquad \text{(Eq 3.39)}$$

$$C_{L_{max_{Std\,\dot{V}}}} = C_{L_{max_{Test}}} \left(\frac{R + 1}{R + 2} \right) \qquad \text{(Eq 3.40)}$$

$$C_{L_{max_{Std\,\dot{V}}}} = C_{L_{max}} + K_d \left[\dot{V}_{Std} - \dot{V}_{Test} \right] \qquad \text{(Eq 3.25)}$$

$$C_{L_{max_{Std\,\dot{V},\,CG}}} = C_{L_{max_{Std\,\dot{V}}}} + K_c \left(CG_{Std} - CG_{Test} \right) \qquad \text{(Eq 3.26)}$$

$$C_{L_{max_{Std\,\dot{V},\,CG,\,W}}} = C_{L_{max_{Std\,\dot{V},\,CG}}} + K_W \left(W_{Std} - W_{Test} \right) \qquad \text{(Eq 3.31)}$$

Where:

$\frac{c}{2}$	Semi-chord length	ft
CG_{Std}	Standard CG	% MAC
CG_{Test}	Test CG	% MAC
$C_{L_{max}}$	Maximum lift coefficient	
$C_{L_{max\ Std\,\dot{V}}}$	Maximum lift coefficient at standard deceleration rate	
$C_{L_{max\ Std\,\dot{V}\,,\,CG}}$	Maximum lift coefficient at standard deceleration rate and CG	
$C_{L_{max\ Std\,\dot{V}\,,\,CG,\,W}}$	Maximum lift coefficient at standard deceleration rate, CG, and weight	
$C_{L_{max_{Test}}}$	Test maximum lift coefficient	
$\Delta H_{P_{ic}}$	Altimeter instrument correction	ft
ΔH_{pos}	Altimeter position error	ft
$\Delta n_{z_{ic}}$	Normal acceleration instrument correction	g
$\Delta n_{z_{tare}}$	Accelerometer tare correction	g

δ_{Test}	Test pressure ratio	
ΔV_{ic}	Airspeed instrument correction	kn
ΔV_{pos}	Airspeed position error	kn
Hp_c	Calibrated pressure altitude	ft
Hp_i	Indicated pressure altitude	ft
Hp_o	Observed pressure altitude	ft
K_d	Slope of $C_{L_{max}}$ vs $\dot{V}$	
K_W	Slope of $C_{L_{max\ Std\ \dot{V},\ CG}}$ vs GW	lb^{-1}
M	Mach number	
n_z	Normal acceleration	g
n_{z_i}	Indicated normal acceleration	g
n_{z_o}	Observed normal acceleration	g
P_{ssl}	Standard sea level pressure	2116.217 psf
R	Number of semi-chord lengths	
S	Wing area	ft^2
V_c	Calibrated airspeed	kn
V_i	Indicated airspeed	kn
V_o	Observed airspeed	kn
$\dot{V}_{Test}$	Test acceleration/deceleration rate	kn/s
W_{Std}	Standard weight	lb
W_{Test}	Test Weight	lb.

From the observed airspeed, pressure altitude, normal acceleration, fuel weight, and deceleration rate, compute C_L as follows:

Step	Parameter	Notation	Formula	Units	Remarks
1	Observed airspeed	Vo		kn	
2	Airspeed instrument correction	ΔV_{ic}		kn	Lab calibration
3	Indicated airspeed	V_i	Eq 3.32	kn	
4	Airspeed position error	ΔV_{pos}		kn	Not required for trailing cone, May not be available for the test airplane

5	Calibrated airspeed	V_c	Eq 3.33	kn	
6	Observed pressure altitude	H_{P_o}		ft	
7	Altimeter instrument correction	$\Delta H_{P_{ic}}$		ft	Lab calibration
8	Indicated pressure altitude	H_{P_i}	Eq 3.34	ft	
9	Altimeter position error	ΔH_{pos}		ft	Not required for trailing cone, May not be available for the test airplane
10	Calibrated pressure altitude	H_{P_c}	Eq 3.35	ft	
11	Mach number	M			From Appendix VIII, using H_{P_c} and V_c
12	Observed normal acceleration	n_{z_o}		g	
13	Normal acceleration instrument correction	$\Delta n_{z_{ic}}$		g	Lab calibration
14	Indicated normal acceleration	n_{z_i}	Eq 3.36	g	
15	Normal acceleration tare correction	$\Delta n_{z_{tare}}$		g	Flight observation
16	Normal acceleration	n_z	Eq 3.37	g	
17	Test weight	W_{Test}		lb	
18	Test pressure ratio	δ_{Test}			From Appendix VI, using H_{P_c}
19	Standard sea level pressure	P_{ssl}		psf	2116.217 psf
20	Wing area	S		ft^2	
21	Test maximum lift coefficient	$C_{L_{max_{Test}}}$	Eq 3.38		
22	Chord length	c		ft	

23	Test deceleration rate	$\dot{V}_{Test}$		kn/s	From airspeed trace, if available; otherwise use the observed value
24	Standard deceleration rate	$\dot{V}_{Std}$		kn/s	From specification; otherwise 1/2 kn/s
25	R parameter	R	Eq 3.39		
26	Slope of $C_{L_{max}}$ vs $\dot{V}$	K_d		kn/s	From graph
27 a	Maximum lift coefficient at standard deceleration rate	$C_{L_{max\ Std\ \dot{V}}}$	Eq 3.40		Empirical correction
27 b	Maximum lift coefficient at standard deceleration rate	$C_{L_{max\ Std\ \dot{V}}}$	Eq 3.25		Graphical correction
28	Test CG	CG_{Test}		% MAC	
29	Standard CG	CG_{Std}		% MAC	From specification
30	Slope of $C_{L_{max\ Std\ \dot{V}}}$ vs CG	K_c			
31	Maximum lift coefficient at standard deceleration rate and CG	$C_{L_{max\ Std\ \dot{V},\ CG}}$	Eq 3.26		Graphical correction.
32	Standard weight	W_{Std}		lb	From specification
33	Slope of $C_{L_{max\ Std\ \dot{V},\ CG}}$ vs GW	K_W		lb^{-1}	
34	Maximum lift coefficient at standard deceleration rate, CG, and weight	$C_{L_{max\ Std\ \dot{V},\ CG,\ W}}$	Eq 3.31		Graphical correction.
35	Maximum lift coefficient at standard deceleration rate, CG, weight, and altitude	$C_{L_{max\ Std\ \dot{V},\ CG,\ W,\ H_P}}$			From $C_{L_{max}}$ versus H_P plot
36	Referred normal acceleration	$n_z \frac{W}{\delta}$		g-lb	Calculation for data presentation

Finally, plot $n_z \frac{W}{\delta}$ versus Mach as shown in figure 3.20 and $C_{L_{max\ Std\ \dot{V},\ CG,\ W}}$ versus H_{P_c} as shown in figure 3.17

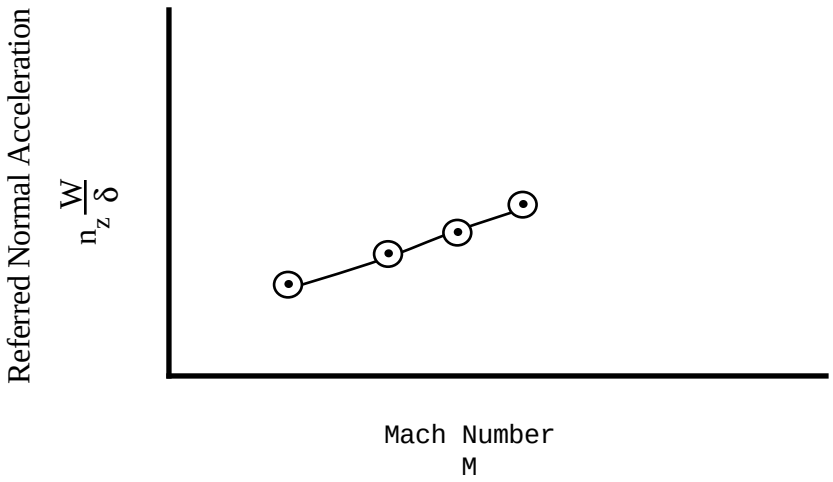

Figure 3.20
REFERRED NORMAL ACCELERATION VERSUS MACH NUMBER

3.5.2 POWER-ON STALLS

The procedure to calculate the lift coefficient for power-on stalls is the same as for power-off stalls. Power effects can be documented when measurements of gross thrust and ram drag are available. The lift from the inclined thrust axis can be accounted for directly. However, the indirect effects of thrust (i.e., flow entrainment and trim lift) are contained in the aerodynamic lift term and can be isolated only by subtracting the aerodynamic lift measured with the power-off. The following procedure is used to calculate the power effects.

Data reduction for power-on stalls is similar to section 3.5.1. The following additional equations are needed:

$$C_{T_G} = \frac{T_G \sin \alpha_j}{q\ S} \qquad \text{(Eq 3.30)}$$

$$\left(C_{L_{aero}}{}_{Std\ \dot{V},\ CG,\ W}\right)_{Pwr\ ON} = \left(C_{L_{max}}{}_{Std\ \dot{V},\ CG,\ W}\right)_{Pwr\ ON} - C_{T_G} \quad \text{(Eq 3.41)}$$

$$\Delta C_{L_t} = \frac{T_G}{q\,S}\left(\frac{Z}{l_t}\right) - \frac{D_R}{q\,S}\left(\frac{Y}{l_t}\right) \quad \text{(Eq 3.28)}$$

$$\left(C_{L_{aero}}{}_{Std\ \dot{V},\ CG,\ W}\right)_{Pwr\ OFF} = \left(C_{L_{aero}}{}_{Std\ \dot{V},\ CG,\ W}\right)_{Pwr\ ON} - \Delta C_{L_t} - \Delta C_{L_E} \quad \text{(Eq 3.42)}$$

Where:

α_j	Thrust angle	deg
C_{D_R}	Coefficient of ram drag	
$\left(C_{L_{aero\ Std\ \dot{V},\ CG,\ W}}\right)_{Pwr\ OFF}$	Aerodynamic lift coefficient at standard deceleration rate, CG, and weight, power-off	
$\left(C_{L_{aero\ Std\ \dot{V},\ CG,\ W}}\right)_{Pwr\ ON}$	Aerodynamic lift coefficient at standard deceleration rate, CG, and weight, power-on	
$\left(C_{L_{max\ Std\ \dot{V},\ CG,\ W}}\right)_{Pwr\ ON}$	Maximum lift coefficient at standard deceleration rate, CG, and weight, power-on	
C_{T_G}	Coefficient of gross thrust lift	
ΔC_{L_E}	Coefficient of thrust-entrainment lift	
ΔC_{L_t}	Incremental tail lift coefficient	
l_t	Moment arm for tail lift	ft
q	Dynamic pressure	psf
S	Wing area	ft^2
T_G	Gross thrust	lb
Y	Height of CG above ram drag	ft
Z	Height of CG above gross thrust.	ft

To calculate the aerodynamic lift coefficient at standard deceleration rate, CG, and weight power-off proceed as follows:

Step	Parameter	Notation	Formula	Units	Remarks
1	Maximum lift coefficient at standard deceleration rate, CG, and weight, power-on	$\left(C_{L_{max\ Std\ \dot{V},\ CG,\ W}}\right)_{Pwr\ ON}$			As for power-off
2	Gross thrust	T_G		lb	From contractor
2	Coefficient of gross thrust lift	C_{T_G}	Eq 3.30		
3	Aerodynamic lift coefficient at standard deceleration rate, CG, and weight, power-on	$\left(C_{L_{aero\ Std\ \dot{V},\ CG,\ W}}\right)_{Pwr\ ON}$	Eq 3.41		
4	Incremental tail lift coefficient	ΔC_{L_t}	Eq 3.28		
5	Coefficient of thrust-entrainment lift	ΔC_{L_E}			From contractor
6	Aerodynamic lift coefficient at standard deceleration rate, CG, and weight, power-off	$\left(C_{L_{aero\ Std\ \dot{V},\ CG,\ W}}\right)_{Pwr\ OFF}$	Eq 3.42		

3.6 DATA ANALYSIS

3.6.1 CALCULATING $C_{L_{MAX}}$ FOR STANDARD CONDITIONS

3.6.1.1 POWER-OFF STALLS

After the data reduction is complete, the corrected values of $C_{L_{max}}$ for standard conditions are known. Values of $C_{L_{max}}$ for other conditions of deceleration rate, gross weight, CG position, or altitude can be calculated using the correction factors determined from the test results, plus the altitude variation graph.

3.6.1.2 POWER-ON STALLS

The procedure recommended to determine the power-on lift coefficient for standard conditions is the following:

1. Calculate $C_{L_{max}}$ with power-off and correct for $\dot{V}$, CG, and W to obtain $\left(C_{L_{max\ Std\ \dot{V},\ CG,\ W}}\right)_{Pwr\ OFF}$.
2. Subtract the thrust effects (C_{T_G}, ΔC_{L_t}, and ΔC_{L_E}) to get $\left(C_{L_{aero\ Std\ \dot{V},\ CG,\ W}}\right)_{Pwr\ OFF}$.
3. Obtain the standard thrust and calculate the corresponding C_{T_G}, ΔC_{L_t}, and ΔC_{L_E}.
4. Add the corrections to $\left(C_{L_{max\ Std\ \dot{V},\ CG,\ W}}\right)_{Pwr\ OFF}$ to get $\left(C_{L_{max\ Std\ \dot{V},\ CG,\ W}}\right)_{Pwr\ ON}$.
5. Plot versus H_{P_c} for the extrapolation to sea level, if required.

3.6.2 CALCULATING STALL SPEED FROM $C_{L_{MAX}}$

Once $C_{L_{max}}$ is determined, the equivalent airspeed of interest can be calculated using Eq 3.43 to solve for V_{e_s}.

$$V_{e_s} = \sqrt{\frac{841.5\ n_z\ W}{C_{L_{max}}\ S}} \qquad \text{(Eq 3.43)}$$

Where:

$C_{L_{max}}$	Maximum lift coefficient	
n_z	Normal acceleration	g
S	Wing area	ft^2
V_{e_s}	Stall equivalent airspeed	kn
W	Weight	lb.

3.7 MISSION SUITABILITY

The stall speed represents the absolute minimum useable speed for an airplane in steady conditions. For takeoff and landing phases, recommended speeds are chosen a safe margin above the stall speeds. For takeoffs the margin depends upon:

1. The stall speed.
2. The speed required for positive rotation.
3. The speed at which thrust available equals thrust required after liftoff.
4. The minimum control speed after engine failure for multi-engine airplanes.

For catapult launches, the minimum speed also depends upon a 20 ft maximum sink limit off the bow. The minimum end speed for launches is intended to give at least a 4 kn margin above the absolute minimum speed. For landing tasks, similar considerations are given to the approach and potential waveoff scenarios. Normally a twenty percent margin over the stall speed (however determined) is used, making the recommended approach speed 1.2 times the stall speed.

From the pilot's perspective, low takeoff speeds are desirable for several reasons. With a low takeoff speed the airplane can accelerate to takeoff speed quickly, using relatively little runway to get airborne. Safety is enhanced since relatively more runway is available for aborting the takeoff in emergencies. Operationally, the short takeoff distance provides flexibility for alternate runway takeoffs (off-duty, downwind, etc.) and allows the airplane to operate from fields with short runways. For shipboard operations, the low takeoff speed is less stressful on the airframe and the ship's catapult systems, and makes it easier to launch in conditions of little natural wind.

Low approach speeds provide relatively more time to assess the approach parameters and make appropriate corrections. The airplane is also more maneuverable at low speeds, since tight turns are possible. Low approach speeds also make the airplane easier to handle from an air traffic control perspective. The air traffic controller can exploit the airplane's speed flexibility for aircraft sequencing and its enhanced maneuverability for vectoring in and around the airfield for departures, circling approaches, and missed approaches.

Low landing speeds give the pilot relatively more time to react to potential adverse runway conditions after touchdown. Less runway is used during the time it takes the pilot to react to a problem and decide to go-around. Low landing speeds also help to reduce the kinetic energy which has to be absorbed during the rollout by the airplane's braking system or by the ship's arresting gear. Low landing speeds promote short stopping distances, leaving more runway ahead and a safety margin in case of problems during the rollout. The reduced runway requirements also give the airplane operational flexibility, as in the takeoff case.

3.8 SPECIFICATION COMPLIANCE

The stall speed is used to verify compliance with performance guarantees of the detailed specification. The specified minimum takeoff and landing speeds are determined using the stall speed as a reference. For example, the minimum approach speed might be specified to be below a certain airspeed for a prescribed set of conditions. The specified approach speed (V_{APR}) may be referenced to a minimum speed in the approach configuration ($V_{PA_{min}}$), with $V_{PA_{min}}$ defined as a multiple of the stall speed (V_S). That is, $V_{APR} = 1.05\ V_{PA_{min}}$, where $V_{PA_{min}} = 1.1\ V_S$. The minimum approach speed, equal to $(1.1)(1.05)V_S$, would meet the specification requirement only if the stall speed was low enough for the identical conditions. Similarly, the takeoff speed specifications depend upon the stall speed in the takeoff configuration.

3.9 GLOSSARY

3.9.1 NOTATIONS

AFCS	Automatic flight control system	
AR	Aspect ratio	
BLC	Boundary layer control	
c	Chord length	ft
$\frac{c}{2}$	Semi-chord length	ft
CAS	Calibrated airspeed	kn
C_{D_R}	Coefficient of ram drag	
CG	Center of gravity	% MAC
CG_{Std}	Standard CG	% MAC

CG_{Test}	Test CG	% MAC
C_L	Lift coefficient	
$C_{L_{aero}}$	Aerodynamic lift coefficient	
$(C_{L_{aero\ Std\ \dot{V},\ CG,\ W}})_{Pwr\ OFF}$	Aerodynamic lift coefficient at standard deceleration rate, CG, and weight, power-off	
$(C_{L_{aero\ Std\ \dot{V},\ CG,\ W}})_{Pwr\ ON}$	Aerodynamic lift coefficient at standard deceleration rate, CG, and weight, power-on	
$C_{L_{max}}$	Maximum lift coefficient	
$C_{L_{max\ (\Lambda = 0)}}$	Maximum lift coefficient at $\Lambda = 0$	
$C_{L_{max\ (\Lambda)}}$	Maximum lift coefficient at Λ wing sweep	
$C_{L_{max\ Std\ \dot{V}}}$	Maximum lift coefficient at standard deceleration rate	
$C_{L_{max\ Std\ \dot{V},\ CG}}$	Maximum lift coefficient at standard deceleration rate and CG	
$C_{L_{max\ Std\ \dot{V},\ CG,\ W}}$	Maximum lift coefficient at standard deceleration rate, CG, and weight	
$(C_{L_{max\ Std\ \dot{V},\ CG,\ W}})_{Pwr\ ON}$	Maximum lift coefficient at standard deceleration rate, CG, and weight, power-on	
$C_{L_{max\ Std\ \dot{V},\ CG,\ W,\ H_P}}$	Maximum lift coefficient at standard deceleration rate, CG, weight, and altitude	
$C_{L_{max_{Test}}}$	Test maximum lift coefficient	
C_{L_s}	Stall lift coefficient	
$C_{L_{Test}}$	Test lift coefficient	
C_{T_G}	Coefficient of gross thrust lift	
D	Drag	lb
ΔC_{L_E}	Coefficient of thrust-entrainment lift	
ΔC_{L_t}	Incremental tail lift coefficient	
$\Delta H_{P_{ic}}$	Altimeter instrument correction	ft
ΔH_{pos}	Altimeter position error	ft
ΔL_t	Tail lift increment	lb
$\Delta n_{z_{ic}}$	Normal acceleration instrument correction	g

$\Delta n_{z_{tare}}$	Accelerometer tare correction	g
D_R	Ram drag	lb
ΔV_{ic}	Airspeed instrument correction	kn
ΔV_{pos}	Airspeed position error	kn
H_P	Pressure altitude	ft
H_{P_c}	Calibrated pressure altitude	ft
H_{P_i}	Indicated pressure altitude	ft
H_{P_o}	Observed pressure altitude	ft
K_c	Slope of $C_{L_{max\ Std\ \dot{V}}}$ vs CG	
K_d	Slope of $C_{L_{max}}$ vs $\dot{V}$	
K_W	Slope of $C_{L_{max\ Std\ \dot{V},\ CG}}$ vs GW	lb^{-1}
L	Lift	lb
l	Length	ft
L_{aero}	Aerodynamic lift	lb
l_t	Moment arm for tail lift	ft
L_{Thrust}	Thrust lift	lb
M	Mach number	
MAC	Mean aerodynamic chord	
N	Engine speed	RPM
n_x	Acceleration along the X axis	g
n_z	Normal acceleration	g
$n_z \frac{W}{\delta}$	Referred normal acceleration	g-lb
n_{z_i}	Indicated normal acceleration	g
n_{z_o}	Observed normal acceleration	g
OAT	Outside air temperature	˚C or ˚K
P_{ssl}	Standard sea level pressure	2116.217 psf
q	Dynamic pressure	psf
R	Number of semi-chord lengths	
R_e	Reynold's number	
S	Wing area	ft^2
T	Thrust	lb
T_G	Gross thrust	lb
V	Velocity	kn
V_{APR}	Approach speed	kn
V_c	Calibrated airspeed	kn

V_e	Equivalent airspeed	kn
V_{e_s}	Stall equivalent airspeed	ft/s or kn
V_i	Indicated airspeed	kn
V_o	Observed airspeed	kn
$V_{PA_{min}}$	Minimum speed in the approach configuration	kn
V_s	Stall speed	kn
$V_{s_{Test}}$	Test stall speed	kn
$\dot{V}$	Acceleration/deceleration rate	kn/s
$\dot{V}_{Std}$	Standard acceleration/deceleration rate	kn/s
$\dot{V}_{Test}$	Test acceleration/deceleration rate	kn/s
W	Weight	lb
W_{Std}	Standard weight	lb
W_{Test}	Test weight	lb
Y	Height of CG above ram drag	ft
Z	Height of CG above gross thrust	ft

3.9.2 GREEK SYMBOLS

α (alpha)	Angle of attack	deg
α_j	Thrust angle	deg
δ (delta)	Pressure ratio	
δ_{Test}	Test pressure ratio	
γ (gamma)	Flight path angle,	
	Ratio of specific heats	deg
Λ (Lambda)	Wing sweep angle	deg
λ (lambda)	Taper ratio	
μ (mu)	Viscosity	lb-s/ft^2
θ (theta)	Pitch attitude	deg
ρ (rho)	Air density	slug/ft^3
ρ_{ssl}	Standard sea level air density	0.0023769 slug/ft^3
τ (tau)	Inclination of the thrust axis with respect to the chord line	deg

3.10 REFERENCES

1. Branch, M., *Determination of Stall Airspeed at Altitude and Sea Level*, Flight Test Division Technical Memorandum, FTTM No. 3-72, Naval Air Test Center, Patuxent River, MD, November, 1972.

2. Federal Aviation Regulations, Part 23, *Airworthiness Standards: Normal, Utility, and Acrobatic Category Airplanes*, June 1974.

3. Lan, C. E., and Roskam, J., *Airplane Aerodynamics and Performance*, Roskam Aviation and Engineering Corp.,Ottawa, Kansas, 1981.

4. Lean, D., *Stalling and the Measurement of Maximum Lift*, AGARD Flight Test Manual, Vol II, Chap 7, Pergamon Press, Inc., New York, NY., 1959.

5. McCue, J.J., *Pitot-Static Systems*, USNTPS Class Notes, USNTPS, Patuxent River, MD., June, 1982.

6. Military Standard, "Flying Qualities of Piloted Aircraft", MIL-STD-1797A, 30 January, 1990.

7. Naval Test Pilot School Flight Test Manual, *Fixed Wing Performance, Theory and Flight Test Techniques*, USNTPS-FTM-No.104, U. S. Naval Test Pilot School, Patuxent River, MD, July, 1977.

8. Powell, J., *Airplane Performance*, USNTPS Classroom Notes, USNTPS, Patuxent River, MD.

9. Strike Aircraft Test Directorate Flight Test Manual, *Carrier Suitability Testing Manual*, SA FTM-01, Strike Aircraft Test Directorate, Patuxent River, MD, March,1991.

10. USAF Test Pilot School, *Performance Phase Textbook Volume I*, USAF-TPS-CUR-86-01, USAF, Edwards AFB, CA, April, 1986.